Eur. Phys. J. Plus (2021) 136:929
https://doi.org/10.1140/epjp/s13360-021-01897-9

THE EUROPEAN PHYSICAL JOURNAL PLUS

Regular Article

Inputs to produce lime mortar for conservation and restoration of Thanjavur Palace, India: characterization study

Matej Dolenec[1], Sabina Dolenec[2], Sriram Pradeep Saridhe[3], Ravi Ramadoss[4], Katarina Šter[2], Thirumalini Selvaraj[3,a]

[1] Faculty of Natural Sciences and Engineering, University of Ljubljana, Askercevaulica 12, 1000 Ljubljana, Slovenia
[2] ZAG - Slovenian National Building and Civil Engineering Institute, dimicevaulica 12, 1000 Ljubljana, Slovenia
[3] Department Structural and Geotechnical Engineering, School of Civil Engineering, Vellore Institute of Technology (VIT), Vellore, Tamil Nadu 632014, India
[4] Department of Civil Engineering, SRM Institute of Science and Technology, kattankulathur, Tamil Nadu 603203, India

Received: 10 May 2021 / Accepted: 25 August 2021

Abstract The present study characterizes mortars from Thanjavur Palace (Thanjavur, India) to illustrate ancient production methods and the raw materials used. The mineralogical-petrographic composition of mortars was determined using optical microscopy, supported by scanning electron microscopy with energy-dispersive spectroscopy and X-ray powder diffraction. The chemical composition and organic content of the binder were also determined. The aggregate-binder ratio and particle size distribution of the mortars were investigated. Results showed that the composition of both the aggregate and binder varied between mortars. The aggregate consisted mainly of quartz, with small quantities of feldspar and individual grains of limestone and other lithic grains present. The majority of the mortars contained a lime binder, but kaolinite was also identified, indicating a clay binder. Kaolinite primarily occurred in bedding mortars rather than plaster mortars. All samples were in a deteriorated state due to the presence of gypsum and halite. Analysis of particle size distribution confirmed the size of the aggregates to range between 1.18 and 0.3 mm, showing that the aggregates must have been ground in order to allow for the dispersion of binders. Furthermore, biomolecules in the form of carbohydrates, proteins and fats, which could serve as natural admixtures to improve properties in both the fresh and hardened state, were identified in all mortar samples.

1 Introduction

Various binders such as clay, bitumen, gypsum and lime have been used since ancient times as a construction material to build and repair old structures such as palaces, temples, churches and forts [1]. Among all the binders mentioned, lime is the most widely used across the world. After the invention of cement in the nineteenth century, the use of lime declined. Since then,

[a] e-mail: p.thirumalini@yahoo.in (corresponding author)

lime has primarily been used for the conservation and restoration of ancient structures, due to incompatibilities between the chemistries of cement and lime [2].

To overcome the problems associated with air lime mortars, such as slow setting and carbonation, low strength, and high drying shrinkage, ancient builders incorporated pozzolans into lime mortars [3]. Pozzolans contain reactive silica/alumina components which interact with free lime and promote the formation of hydraulic phases. Initially, the Romans added reactive sand (volcanic ash) extracted from Mount Vesuvius to impart hydraulic character. The use of pozzolanic materials in lime mortars used for the construction of drainage canals has been observed dating back to 400 B.C [4]. The strength and durability of lime binders are also improved by the addition of mineral additives in the form of brick powder [5]. These special mortars and plasters were mainly used in Roman times for the construction of aqueducts, bridges, and bathing buildings, where waterproofing was required [6].

The Romans built durable and efficient concrete harbors along the central Italian coast, which still stand after 2000 years, despite constant exposure to seawater. The reason for such longevity is their wise choice of raw materials and installation methods. They achieved a robust mix by blending lime, volcanic ash and zeolite chunks with seawater, resulting in a durable phase, similar to calcium silica-alumina hydrates and Al-rich tobermorite [7–9]. Where natural pozzolan was not available, the Romans developed hydraulic mortars by blending lime with crushed bricks [10]. The amorphous phases on the brick particles interact with free lime and initiate the formation of hydraulic phases such as calcium silica/aluminate hydrates [6, 11–14].

More recently, researchers found beneficial results following the addition of calcined clay minerals to lime mortars, including faster setting and improved waterproofing properties [11]. Vejmelkova et al. [15] investigated the behavior of clay shale as a pozzolan in lime mortars and concluded that this combination could be useful for the conservation–restoration of lime pozzolan mortars. Furthermore, the interaction of lime-metakaolin mortars and their applicability in the conservation–restoration of ancient masonries has been investigated [3]. Arizzi and Cultrone [3] co-related the performance of air lime and lime pozzolan mortars. By replacing 10% of metakaolin in lime mortars, the authors achieved grater compatibility with aerial lime mortars with respect to physical and mechanical properties.

In addition to mineral additives, chemical admixtures in the form of plant and animal extracts have been used in lime mortars worldwide [16, 17]. The addition of chemical admixtures improves properties such as hardness, adhesion, setting and impermeability in lime mortars. Sticky rice is one such chemical admixture, which has been widely used in important structures, e.g., harbors, and other significant monuments such as the Great Wall of China [18]. Yang et al. [19] have studied the interaction of sticky rice with lime mortars and concluded that, amylopectin, an organic compound contained in sticky rice, acts as a crystal growth inhibitor and encouraged the precipitation of amorphous calcium carbonate rather than calcite. In general, the precipitation of calcium carbonate highly depends upon the factors such as pH, temperature, and degree of supersaturation [20]. To support this, Zeng et al. [21] investigated the crystal precipitation of calcium carbonate in sticky rice loaded lime mortar through morphological studies (SEM analysis); the distinct variation in precipitation of calcium carbonates is observed. In sticky rice blended mortar, the calcium carbonate has attained the compact micro-structure (in the form spherical), whereas the reference mortars have displayed regular cubic shape of calcium carbonate. Authors have claimed that the developed compact structure has improved the properties of lime mortars.

A combination of Tung oil–lime mortar is an organic–inorganic binder used in structures which are likely to be exposed to humid environments. This combination also helps to improve the mechanical and weathering properties of lime mortars [22]. The use of linseed in lime

mortars has also been shown to improve hydrophobicity and reduce water absorption and salt crystallization in lime mortars [23]. Ventola et al. [24] investigated the role of polysaccharides, proteins and fats in lime mortars and concluded that polysaccharides contribute to an increase in the carbonation, proteins double the compressive strength, and fats reduce their porosity.

To improve the strength and durability of lime mortar, most ancient structures in India were constructed with the addition of naturalpolymers in the form of fermented plant extracts [25, 26]. Nene [27] discussed various fermented plant extracts that were used in the construction of ancient structures in India, including jaggery, kadukkai, black gram seeds, bel fruit, and cactus [28]. Among the various plant extracts used in ancient structures, fermented jaggery and kadukkai have been extensively used throughout India. During fermentation, these plant extracts transform into short-chain alcohols interaction of these alcohols with lime results in the formation of metastable vaterite instead of calcite, and improves the longevity of the mortars [26, 29]. The addition of fermented cactus also has many advantages, including providing sufficient moisture in the lime matrix for better carbonation and improving properties of strength and durability [30]. Various plant extracts including jaggery (unrefined sugar), kadukkai (Terminalia chebula), oonjalvali (Cissus glauca Roxb), kulamavu (Perseama crantha), and pananchikaai (cochlospermum religiosum) have been found in lime mortars at the ancient Vadakumnathan temple in Kerala, India [31]. The fermented plant extracts used have been found to be rich in carbohydrates, proteins and fats, which acted as natural polymers to improve the performance of the lime mortars. In India, the selection of plant extracts varies by region, but in most cases ancient builders chose carbohydrate-rich fermented plant extracts to enhance the properties of lime mortars [28, 29].

The main limitations when formulating mortar compatible for repair work are the types of binder (clay, gypsum, or lime, either air or hydraulically mixed) and aggregate (reactive/non-reactive), the binder/aggregate ratio, and the admixtures used. Ancient materials can be characterized by consolidating results from analytical techniques such as XRD (X-ray diffraction), TGA (thermogravimetric analysis), FT-IR (Fourier transform- infrared spectroscopy), FE/SEM (field emission scanning electron microscopy) and other methods. The application of these different analytical methods gives an indication of the technologies of ancient construction, as well as the raw materials which were selected. In particular, a combination of microscopy and XRD analysis can provide more precise information regarding the physical and mineralogical aspects of both binders and aggregates.

In this study the petrological–mineralogical, chemical, and microstructural compositions of mortar samples from the sixteenth century Thanjavur Palace (Thanjavur, Tamil Nadu, India) were investigated. The petrological–mineralogical compositions of both the aggregate and binder were determined by optical and electron microscopy and X-ray powder diffraction. Additionally, the chemical composition of the binder was determined by wet chemical analyses. The organic components were also identified. Furthermore, the aggregate to binder ratio was determined using an acid digestion test, and sieve analysis was carried out to investigate the particle size distribution. The results will be incorporated into the restoration–conservation intervention at the Thanjavur Palace.

2 Experimental

2.1 Sampling

A total of 15 mortar samples were collected from various locations at the Thanjavur Palace, Thanjavur, Tamil Nadu, India (Fig. 1, 2, 3).

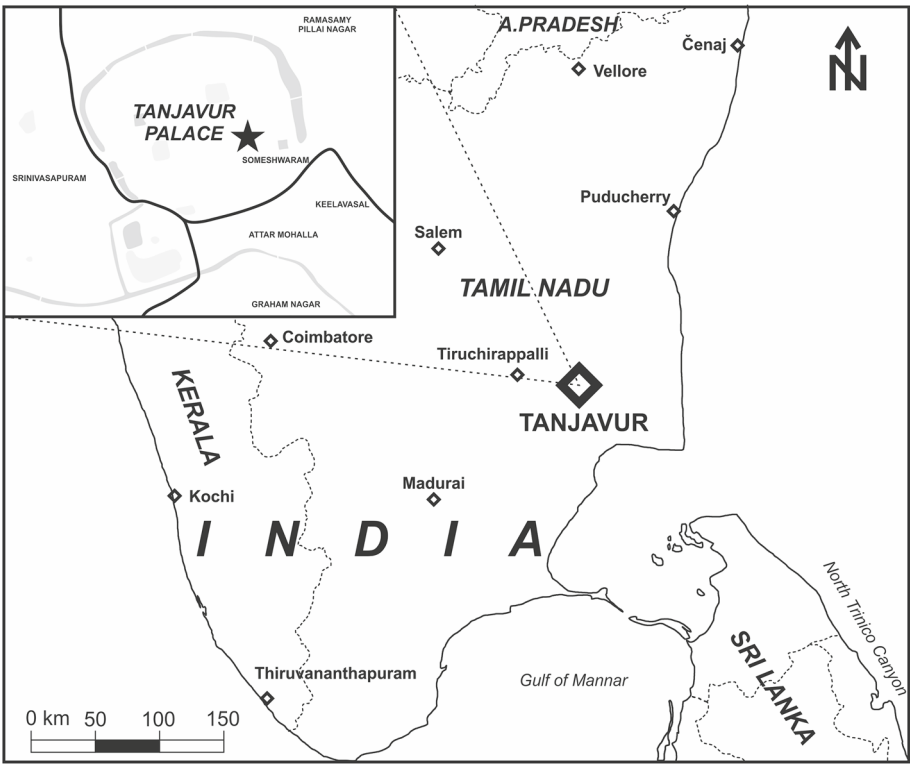

Fig. 1 Location of Thanjavur Palace, India

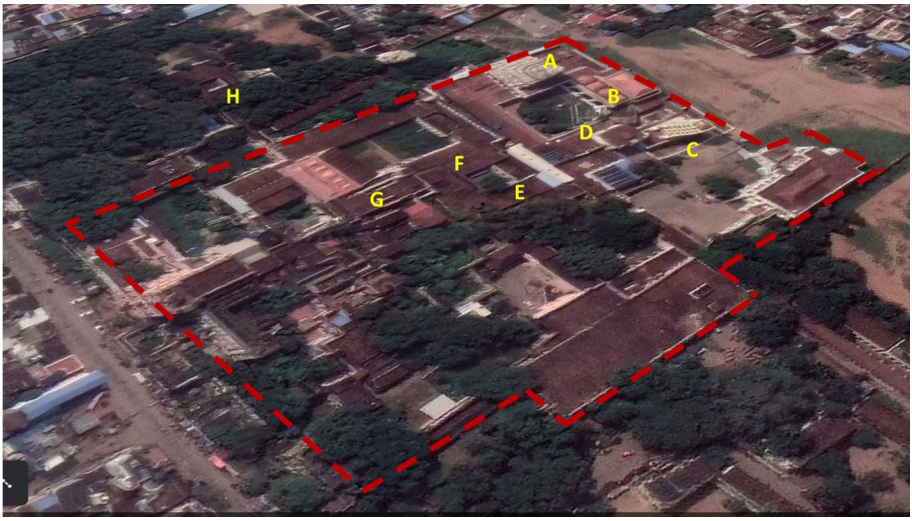

Fig. 2 Aerial view of Thanjavur Palace

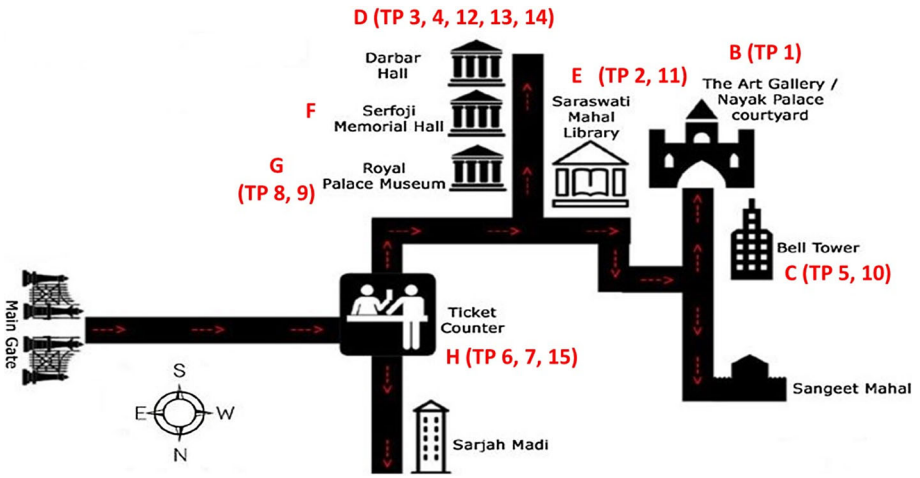

Fig. 3 Sampling points

The Thanjavur Palace was built in 1535 A.D. by the people of Nayak kingdom. Later, in 1674 AD, the palace was taken by the Maratha kings, who extended the palace several times, and in 1799 AD it was incorporated into British territory. At present, the palace complex is maintained by the State Archaeological Department of Tamil Nadu, India. The palace complex consists of various substructures, including the Arsenal Tower, the Bell Tower (Fig. 4), the Maratha Durbar Hall and Saraswathi Mahal. The Arsenal Tower, a pyramid-like construction used by the military for storing weapons and ammunition is 58 m high. The bell tower has exactly the same style as the Arsenal Tower, similar to modern buildings. The Maratha durbar hall (Fig. 5) was used by the Maratha kings as a royal court hall. A rare collection of photographs, coins, and a few mediaeval manuscripts in various languages (Tamil, Telugu, Marathi, Sanskrit etc.) are exhibited in Saraswathi Mahal, which is considered one of the most remarkable ancient libraries of India (Fig. 6).

Information regarding the mortar samples investigated is given in Table 1. The individual sampling points are linked with the map of Thanjavur Palace (Fig. 2 and 3). The samples included clay, plaster, and bedding mortar are collected from across the structure to give a representation of the entire palace. The entire structure consists of brick masonry, so when sampling we avoided mortars that were very close to the surface of the brick. Care was taken to ensure that the entire structure was considered for the study.

2.2 Methods

In order to characterize the mortar samples, and to define the type and content of particular aggregate grains, binder type, and the aggregate to binder ratios, our first approach was to examine thin polished sections of the mortars by means of optical microscopy, using a ZEISS AX 10 microscope equipped with a digital camera (AxioCam MRc5).

The chemical composition of any areas of interest with in the polished thin sections of mortar samples was examined using the back-scattered electrons (BSE) image mode of a low vacuum scanning electron microscope (SEM) and energy-dispersive X-ray spectroscopy (EDS) using a JEOL 5500 LV.

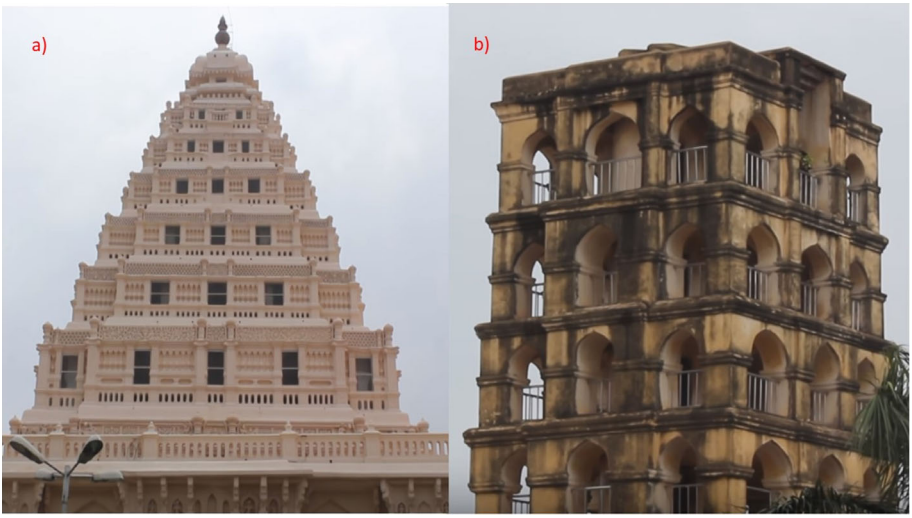

Figure. 4 **a** Arsenal tower. **b** Bell tower

Fig. 5 **a**, **b** Interior of Durbar hall

Phase composition of the mortars was determined on both aggregate and binder-enriched fractions. In order to avoid destroying the aggregate particles, the mortars were gently crushed in order to separate them into fractions of binder and aggregate. The remaining fractions were then sieved through a mesh less than 65 μm in size (XRD performed on mechanically separated binder enriched fraction). The ground powder was manually back-loaded into a circular sample holder (diameter 16 mm) and analyzed by X-ray powder diffraction (XRD) using a PAN analytical Empyrean X-ray diffractometer in Bragg–Brentano θ-θ geometry with a 240 mm goniometer radius and a Cu $K\alpha_1$ radiation of ($\lambda = 1.54$ Å) using 40 mA and 45 kV tube operating conditions. An incident beam and receiving Soller slits of 0.04 rad were used, with fixed divergence and anti-scatter slits. Data was collected over the range 4–70° 2θ with a step size of 0.026°2θ and scan speed of 1°/min, using a spinning sample stage and PIX cell 1D detector. The X-ray diffraction patterns obtained were analyzed using X'Pert High Score Plus diffraction software v. 4.8 from PANalytical, using PAN ICSD v.

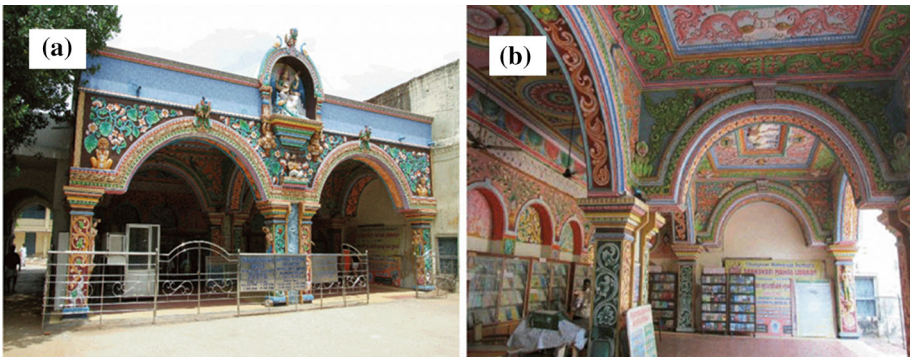

Fig. 6 **a**, **b** Saraswathi Mahal

Table 1 Overview of the mortar samples investigated

Sample	Type of mortar	Sampling points		Structure name
T.P-1	Mud mortar	Back to Amman Statue, indoor	B	Art gallery
T.P-2	Bedding mortar	Near Library, outdoor	E	Saraswathi Mahal library
T.P-3	Plaster mortar	Durbar entrance, indoor	D	Durbar hall
T.P-4	Bedding mortar	Arch/Durbar Hall, indoor	D	Durbar hall
T.P-5	Bedding mortar	Belltower/First floor, indoor	C	Bell tower
T.P-6	Bedding mortar	Elephant ting place, outdoor	H	Ticket counter
T.P-7	Plaster mortar	Arch/Ticket counter, outdoor	H	Ticket counter
T.P-8	Plaster mortar	Museum entrance, outdoor	G	Maratha palace museum
T.P-9	Plaster mortar	Sidewall, outdoor	G	Maratha palace museum
T.P-10	Plaster mortar	Belltower/Outerwall, outdoor	C	Bell tower
T.P-11	Bedding mortar	Library entrance, outdoor	E	Saraswathi Mahal library
T.P-12	Bedding mortar	North wall/Durbar hall, outdoor	D	Durbar hall
T.P-13	Plaster mortar	Inner wall/, indoor	D	Durbar hall
T.P-14	Plaster mortar	First floor/Durbar hall, indoor	D	Durbar hall
T.P-15	Plaster mortar	Inside arch/Ticket counter, indoor	H	Ticket counter

3.4 powder diffraction files. All Rietveld refinements were performed using the PANalytical X'Pert High Score Plus diffraction software, Pseudo Voigt profile function and Chebishev I background method, using phase structures from the ICSD Database FIZ Karlsruhe, version number 2.3.

An acid loss test was conducted to segregate the aggregates from the part enriched with binder, as per the method set out by the RILEM Technical Committee-167 [32]. Initially, 10 g of the crushed mortar sample was dissolved in 200 ml of distilled water. 30 ml of hydrochloricacid was then added and the mixture uniformly stirred for 30 min. Carbonated lime binder dissolves in acid, whereas aggregate settles at the bottom of the container. The aggregate was removed from the bottom, washed several times using distilled water, and then measured in terms of the weight of sand. The part dissolved in acid was filtered through filter paper to separate the binder from the acid, and the weight of binder and aggregates was

calculated. The binder-rich part was taken for chemical analysis, and particle size distribution was determined following sieve analysis of the aggregate.

Chemical analysis was used to determine the concentrations of the oxide compositions of CaO, MgO, Al_2O_3, SiO_2, Fe_2O_3 Na_2O, K_2O, and $SO_4{}^{2-}$ from the filtrate (binder-part) of the acid digestion solution. Normally, the type of binder lime incorporated in ancient structures is very important for restoration purpose and that can be distinguished with the help of Hydraulic Index (HI) and Cementitious Index (CI) [31]. Taylor [33], and Eckel [34] have developed Eqs. (1) & (2) along with the ranges. Based on the oxide compositions, the ranges could be calculated for the binder and can be categorized as either air lime or hydraulic lime.

$$\text{HydraulicIndex(HI)} = \frac{Al_2O_3 + Fe_2O_3 + SiO_2}{CaO + MgO} \tag{1}$$

$$\text{CementationIndex(CI)} = \frac{1.1Al_2O_3 + 0.7Fe_2O_3 + 2.8SiO_2}{CaO + MgO} \tag{2}$$

Identification of lime based on hydraulic index (HI) developed by (Taylor, 1997) [33]

$0.30 < HI < 0.50$ – weakly hydraulic
$0.50 < HI < 0.70$ – moderately hydraulic
$0.70 < HI < 1.10$ – higher the index, more hydraulic properties

Identification of lime based on Cementation Index (CI) developed by (Eckel 1928) [34]

$CI < 0.15$ – air lime
$0.15 < CI < 0.30$ – sub hydraulic Lime
$0.30 < CI < 0.50$ – weakly Hydraulic
$0.50 < CI < 0.70$ – moderately Hydraulic
$0.70 < CI < 1.10$ – higher the index, more hydraulic properties

Loss on ignition was calculated by heating a sample of the material to 400 °C, allowing volatile substances to escape, until its mass ceased to change. This process accounts for the presence of organics in ancient extracts.

Sieve analysis was conducted on the residue collected at the bottom of the acid digestion container to establish the particle size distribution of the aggregate according to Indian standards IS 2386 (Part–I)—1975 [35]. A sieve shaker consisting of a set of sieves including the following sizes was used: 2.36 mm, 1.18 mm, 0.60 mm, 0.30 mm and 0.075 mm. Approximately 20 g of material was sieved for 10 min. Individual fractions were weighed, and the residue was plotted on a semi log graph.

The amount of protein and fat present in the binder (mechanically separated) was quantified using the Kjeldahl and crude fat methods, while the percentage of carbohydrate was calculated based on the percentage of proteinandfat, according to IS 7874 (Part—I)—1975 [36]. In general, the Kjeldahl method is preferred to quantify the amount of protein present in the polymer in the form of nitrogen concentration. To find the protein, the Kjeldahl method involves three major steps, digestion, neutralization and titration. In the first step, the sample is distilled in highly concentrate sulfuric acid, converting amine nitrogen to ammonium ions. During neutralization, the ammonium ions are converted into ammonia gas as a result of heating and distillation. Finally, the amount of protein is calculated by multiplying % nitrogen by 6.25 [31].

The crude fat method is employed to determine the amount of fat content present in the organics. Finally, the percentage of carbohydrate present in the organic materials was calculated using Eq. (3).

$$\text{Total carbohydrate percentage} = (100 - (\text{A} + \text{B} + \text{C} + \text{D})) \tag{3}$$

where A is the percentage by mass of moisture, B is the total percentage by mass of protein, C is the percentage by mass of fat, and D is the total percentage by mass of ash.

3 Results and discussion

3.1 Microscopical analyses

The results of optical microscopy showed that the aggregate of the mortar samples examined was mostly moderately sorted, followed by moderately to poorly sorted and well sorted grains. The aggregate grains appeared in rounded, sub-angular and angular shapes, with sub-rounded grains predominating. The grains are either very isometric, isometric, semi-isometric or semi-elongated. The grain size of the aggregate in the samples investigated varied between 0.05 and 2.1 mm.

The mineralogical-petrographic composition of aggregates was quite similar between the bedding and plaster/rendering mortars. According to microscopic analysis, the aggregate of the mortars examined contained predominantly quartz grains, followed by feldspars (orthoclase, plagioclase, microcline), limestone and lithic grains (Fig. 7). Individual grains of amphibole were also observed. EDS analyses showed that the amphibole grains consisted of Ca, Si, Al, Mg, and Fe, indicating a horn blende mineral.

Quartz grains (mainly monocrystalline with a few polycrystalline grains) were the predominant aggregate of the mud mortar (T.P-1), followed by feldspar (plagioclase, microcline) and individual carbonate grains (microsparitic limestone), Fe-oxides/hydroxides and amphibole. The aggregate grains, which were 0.05–0.76 mm in size (0.03 mm on average), were moderately sorted, angular to rounded with predominant sub-angular grains, isometric to semi-elongated with predominant semi-isometric grains.

The mineralogical-petrographic composition of the bedding mortar aggregates (T.P-2, T.P-4–6, and T.P-11,12) did not differ significantly between samples. Quartz (monocrystalline grains predominate, individual polycrystalline grains) was a predominant component of the aggregate in all samples. Individual quartz crystals in polycrystalline grains were recrystallized, indicating slightly metamorphosed felsic igneous rocks. In addition, ductile deformed quartz grains were observed. Feldspar grains (plagioclases, microcline) were present in smaller amounts, in some samples (e.g., T.P-2 and T.P-4) sericitization and kaolinization of feldspar grains were observed, and some grains were limonitised. Haneefa et al. [37] discussed the geochemistry of lime mortars. They found that, if exposed to natural weathering, environmental fluids can enter pores in the lime mortar and alter the mineral composition. Alongside individual carbonate grains (microsparitic limestone, coarse-grained calcite), grains and epidote grains. In the T.P-6 sample aggregate grains are moderately sorted, with well to moderately sorted grains, which are angular to rounded with predominant sub-rounded or sub-angular grains, isometric to elongated with prevailing semi-isometric grains. The grain size varied between 0.6 and 2.1 mm (from 0.3 to 0.75 mm on average), with individual grains up to 3 mm in size exist. The grain size in the T.P-4 and T.P-12 samples, however, both taken from Durbar hall, is larger than other samples within the group. This may be

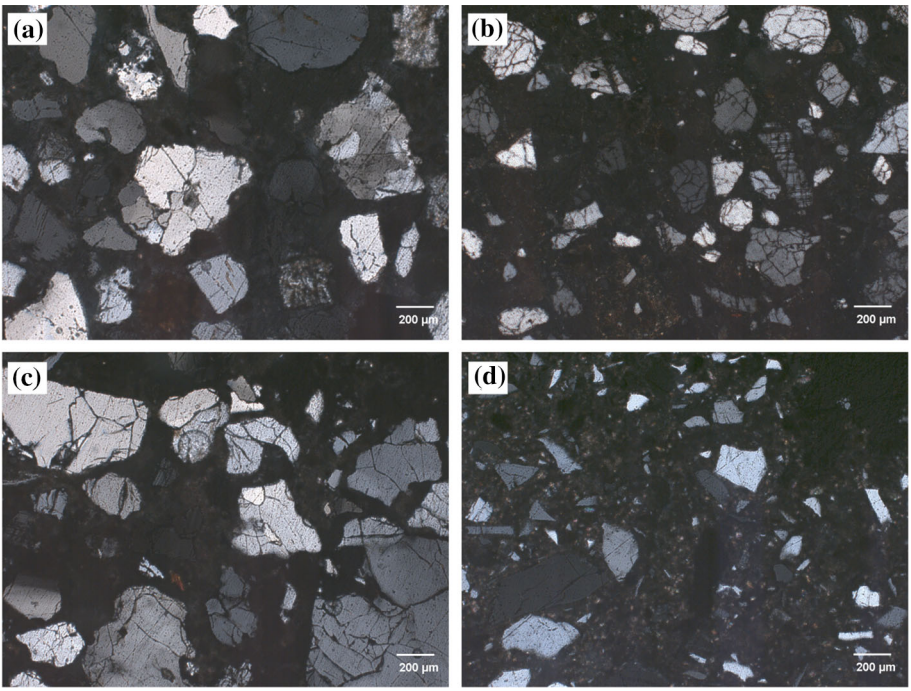

Fig. 7 Photomicrographs of polished thin sections of the samples. **a** Plaster mortar T.P-3, **b** bedding mortar T.P-5, **c** bedding mortar T.P-12, and **d** plaster mortar T.P-15, showing prevailing grains of quartz (*transmitted light, crossed pollars*)

due to the change inconstruction phase, as Durbar Hall was built during the Maratha Period (1674–1855), while the rest of the palace was built earlier by the Nayak Kings (1565–1736).

Quartz, monocrystalline with individual polycrystalline grains, is also a predominant component of the aggregate in the plastering and rendering mortars (samples T.P-3, T.P-7−10, and T.P-13-15). Metamorphic quartz was detected. Feldspar grains (plagioclase, microcline) were present in small amounts, and sericitization and kaolinization of the feldspar grains were observed in some samples (T.P-13). Individual grains of microsparitic limestone, coarse-grained calcite, amphibole, epidote with clinozoisite, and lithic grains were also identified. Limonitised grains with organic matter were observed. The T.P-15 sample differs from others, however, as it contains larger amounts of smaller carbonate grains (~ 0.05 mm in size). Aggregate grains are moderately sorted and moderately to poorly sorted, rounded to angular, with prevailing sub-rounded grains, isometric to elongated with predominantly semi-isometric grains. The grain size varied between 0.5 and 2.3 mm (0.25–0.5 mm on average), with samples T.P-13 and T.P-15 containing the smallest grains.

The mineralogical-petrographic composition of the aggregate indicates that all types of mortar had a similar origin. The mineralogical-petrographic assemblage indicates that the aggregate with the geological background was used in felsic rock. The Thanjavur region primarily consists of Phanerozoic sedimentary rocks, mainly along the coastal belt but also in a river valley inland. Crystalline rocks from the Archaean to the late Proterozoic age occupy over 80% of the area, while the rest is covered by Phanerozoic sedimentary rocks. In the western part of the area, exposures of crystalline rock from the Archaean to the late

Proterozoic age can be seen, also known as crystalline basement rocks. They consist mainly of gneisses, schists, granites and charnockites, which are intruded in places by pegmatite veins [38]. One exception is the T.P-15 sample, in which a larger amount of calcite grains was observed, probably indicating the addition of calcite powder to the mixture. However, the mural paintings are done on the walls at this sampling site, which were executed at a later stage and reworked by the Maratha kings.

The majority of the mortars used lime as a binder, but clay binders were also identified in some samples. Figure 8a shows limonitised binder and EDS analysis of the binder in the T.P-1 sample, which shows the presence of Al and Si, indicating kaolinite and application of mud mortar in the monument.

With the exception of the T.P-12 sample, carbonated lime lumps (0.2–1.3 mm in size) were observed in all the bedding mortar samples. Lime binder was identified in the majority of samples. As shown in the EDS analyses, the binders generally consisted of Ca in the greatest amounts, followed by Si, while smaller amounts of Al, Fe, Mg, Cl, Na and K were also identified (Fig. 8b). Lumps of clay were observed in the T.P-5 sample, however, while lumps of clay with kaolinite were abundant in the T.P-11 sample. On the other hand, large gypsum crystals were observed in some parts of the T.P-6 sample (Fig. 8c).

With the exception of the T.P-3 and T.P-9 samples, lime lumps were also observed in the majority of the plaster and rendering mortar samples, ranging from 0.2 to 1.2 mm in size and larger in some samples (T.P-13 up to 3 mm and T.P-14 up to 5 mm (Fig. 8d). Similar to bedding mortar samples, the lime binder consisted of Cain the greatest amount, followed by Si, then traces of Al, Fe, Mg, Cl, Na and K. Dissolution of the binder and precipitation of secondary calcite grains (Fig. 8e) was seen in the T.P-9 and T.P-11 samples, as a result of variations in humidity due to the environment. The change in humidity conditions in fact triggered precipitation of calcium carbonate along the cracks and voids of lime mortars [36] [39].

3.2 X-ray powder diffraction analysis

The crystalline phases of the identified mortar samples are shown in Table 2 for the aggregate fraction and Table 3 for the binder-enriched fraction. The results of the XRD analysis (Table 2) indicate that quartz, feldspars (plagioclase, K-feldspar) and calcite were the main mineralogical components of all samples examined. The presence of amphiboles, kaolinite, gypsum, halite and mullite was also confirmed.

With regard to the aggregate fraction, quartz and feldspars (Na-Ca plagioclase, K-feldspar) predominate in the mud mortar (T.P-1), followed by amphibole and calcite, all of which are related to the aggregate. The presence of mullite could, however, be due to the brick masonry. Kaolinite has also been identified, indicating the use of a clay binder, as also observed by optical microscopy. Gypsum and halite were present in minor amounts. The predominant phases in the bedding mortar samples were quartz, calcite and feldspars (Na-Ca plagioclases, K-feldspar) followed by, in smaller amounts, amphiboles and mullite. Elevated values of kaolinite were identified for the T.P-5 sample, which is consistent with the microscopic observations. Gypsum was identified in smaller amounts in all samples, the crystalline phases identified in the mortar samples are shown in Tables 2 and 3 for the aggregate fraction and the binder-enriched fraction, respectively. With the exception of the T.P-5 sample, halite was observed in a minor amount in all samples within the group. Similarly, quartz, feldspars and calcite were predominant phases in the plastering mortars, while amphibole, mullite, gypsum and halite were found in minor amounts. Kaolinite was detected in some samples (T.P-10, 13 and 15), probably related to the deterioration of feldspars.

Table 2 Phase composition of the aggregate fraction of the mortar samples investigated, as determined by Rietveld methods: Qtz-quartz, Cal-calcite, Pl-plagioclase, Kfs-K-feldspar, Am-amphibole, Gp-gypsum, Kln-kaolinite, Mul-mullite, and Hl-halite

Sample	Qtz (%)	Cal	Pl	Kfs	Am	Gp	Kln	Mul	Hl
Mud mortar									
T.P-1-R	72.1	0.3	16.1	3.9	1.2	1.9	4.0	0.1	0.3
Bedding mortars									
T.P-2-R	58.0	9.8	20.5	7.4	1.6	1.0	0.4	1.1	0.1
T.P-4-R	61.1	12.7	15.2	7.1	1.4	1.2	0.3	0.9	0.1
T.P-5-R	66.0	17.5	10.3	0.7	1.1	1.6	2.2	0.5	0.0
T.P-6-R	53.8	7.8	20.6	9.1	1.5	6.6	0.0	0.4	0.2
T.P-11-R	63.0	15.2	15.0	2.8	1.4	1.5	0.5	0.5	0.1
T.P-12-R	64.8	7.5	18.1	6.3	1.3	1.1	0.0	0.5	0.4
Plastering mortars									
T.P-3-R	64.5	3.9	19.0	8.5	1.1	1.5	0.0	0.9	0.6
T.P-7-R	52.3	18.0	19.0	6.6	1.5	1.2	0.0	0.8	0.6
T.P-8-R	65.1	3.0	20.6	7.7	1.5	1.3	0.0	0.7	0.2
T.P-9-R	45.9	15.8	22.6	10.9	1.9	1.5	0.0	0.5	0.9
T.P-10-R	55.7	22.1	15.8	1.5	1.6	1.7	0.5	0.7	0.4
T.P-13-R	56.3	18.2	18.5	2.8	1.5	1.3	0.4	0.5	0.5
T.P-14-R	54.2	15.6	20.0	7.2	1.4	1.0	0.0	0.5	0.1
T.P-15-R	50.2	22.6	16.8	5.9	1.6	1.5	0.2	0.5	0.8

Table 3 Phase composition of the binder-enriched fraction of the mortar samples investigated, as defined by Rietveld method. Qtz-quartz, Cal-calcite, Pl-plagioclase, Kfs-K-feldspar, Gp-gypsum, Kln-kaolinite, Mul-mullite, Hl-halite

Sample	Qtz (%)	Cal	Pl	Kfs	Am	Gp	Kln	Mul	Hl
Mud mortar									
T.P-1-P	22.4	6.3	4.0	1.8	0.2	10.7	53.7	0.0	0.8
Bedding mortars									
T.P-2-P	8.8	81.3	4.5	0.8	1.7	1.5	1.4	0.0	0.1
T.P-4-P	8.4	82.1	4.2	0.7	1.7	1.5	1.3	0.0	0.2
T.P-5-P	26.1	53.6	1.5	0.0	0.0	3.8	14.9	0.0	0.0
T.P-6-P	8.4	63.7	11.4	1.0	1.2	11.5	0.2	0.0	2.6
T.P-11-P	12.6	67.3	13.9	0.7	2.3	1.6	1.3	0.0	0.2
T.P-12-P	5.3	81.4	5.2	1.0	1.8	1.6	0.0	0.6	3.0
Plastering mortars									
T.P-3-P	5.9	77.6	7.6	0.9	1.6	1.8	1.2	0.0	3.5
T.P-7-P	2.9	88.2	3.3	0.7	1.5	1.1	0.0	0.0	2.3
T.P-8-P	8.2	71.2	12.3	2.2	1.5	1.9	0.0	0.1	2.7
T.P-9-P	13.2	48.4	27.8	3.1	2.8	2.2	0.0	0.0	2.5
T.P-10-P	8.6	82.4	3.6	0.6	2.2	2.3	0.1	0.0	0.3
T.P-13-P	6.8	81.6	3.8	1.0	1.6	2.0	0.4	0.0	2.6
T.P-14-P	2.7	92.7	1.6	0.5	1.2	1.0	0.0	0.0	0.2
T.P-15-P	5.2	84.9	3.2	0.6	1.3	1.5	0.5	0.0	2.9

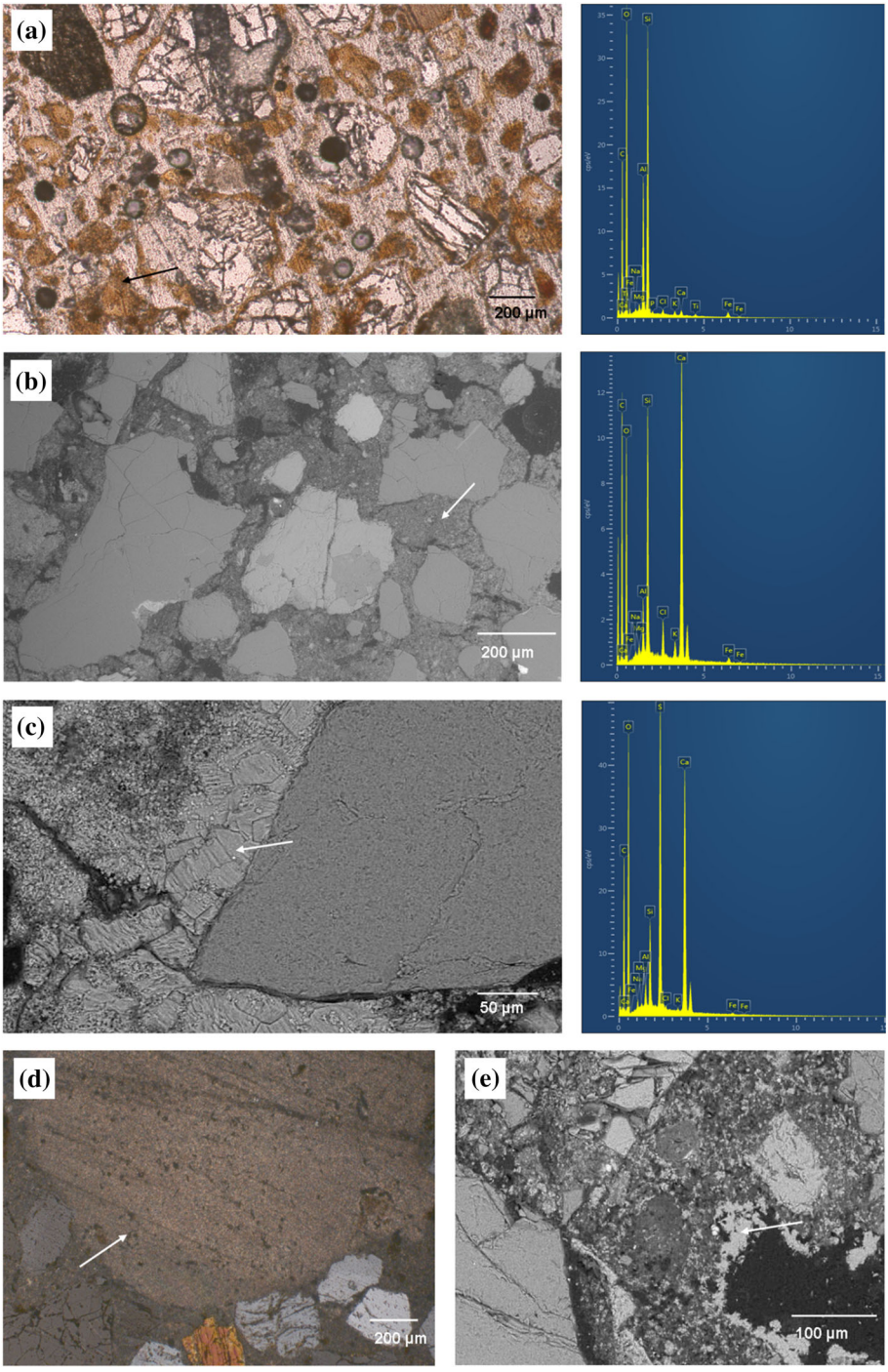

Fig. 8 **a** Clay binder in transmitted light (parallel polar) and EDS analysis indicating kaolinite (sample T.P-1). **b** SEM/BSE microphotographs of bedding mortar sample T.P-12, alongside the EDS spectrum of the binder. **c** SEM/BSE microphotographs of gypsum crystals around the aggregate grain, as results of soluble salt crystallization in bedding mortar sample T.P-6. **d** Lime lump in the T.P-4 plaster mortar sample; transmitted light, crossed polar. **e** SEM/BSE microphotographs showing the dissolution of binder and precipitation of secondary calcite in plaster sample T.P-9

Compared to the aggregate fraction, the binder-enriched fraction contained increased levels of calcite, while Na-Ca plagioclases and quartz were identified in lower amounts. Calcite is related to the carbonated lime binder of mortars. Kaolinite predominated in mud mortar (T.P-1), indicating the use of a clay binder, which is consistent with microscopic analyses. An increased amount of gypsum was also present in this sample, however, except in sample TP6, where a greater amount was observed. The binder-enriched fraction of bedding mortars predominantly consisted of calcite, which is mainly due to the binder, as carbonate grains were observed microscopically only to a small extent. Quartz, feldspars and amphibole were also present as a result of the fine aggregate fraction. Mullite was only identified in the T.P-12 sample. Gypsum was present in all samples, although the values in the T.P-6 sample were rather elevated. Halite was also present in increased concentrations in samples T.P-6 and T.P-12. On the other hand, kaolinite was present in larger amounts in the T.P-5 sample, which shows the addition of clay impurities in the bedding mortar—this site probably represents the oldest of all the lime mortar samples investigated. Aside from T.P-5, traces of kaolinite were observed in all other bedding mortar samples.

The binder-enriched fraction of the plaster samples showed calcite as the main mineral phase, with quartz, minerals of the feldspar group, amphibole, gypsum, halite and traces of kaolinite and mullite present.

The presence of gypsum varied between 1.0 and 2.3%. Compared to the bedding mortars, the plaster samples showed greater precipitation of halite. The proportion of kaolinite in plaster mortars can also be described as minimal. The dominance of calcite represents the complete carbonation of lime mortars. The T.P-5 sample showed elevated values of kaolinite, which shows the addition of clay impurities in the bedding mortar, and this site probably represents the oldest lime mortar sample which was found in other samples only in minor amounts. In general, the bedding mortars are not exposed much to atmospheric carbon dioxide, which prolongs the initial hardening of the lime through carbonation. In India, an impure form of lime with around 30% clay impurities is generally used to improve setting behavior, and these clay minerals help to improve the pozzolanic activity of material and enhance the properties. The XRD, however, did not detect any strength-giving phases (CSH/CASH). Normally, the hardened system of the lime mortar matrix consists of aggregate and lime with well-interconnected pores. As the structure was built in the sixteenth century, the strength-enhancing phases CSH/CASH are carbonated to calcium carbonate due to the continuous carbonation phenomenon [31]. Apart from T.P-5, the other samples also showed traces of kaolinite in all bedding mortars. The largest amount of gypsum and halite among the samples was found in T.P-6. This sample could have been affected by the interaction of any strength-enhancing phases of foreign compounds such as chlorides and sulfates in the environment, which was confirmed by the binder to aggregate ratio. The presence of gypsum was detected in all samples (T.P-2, 4, 11, 12). Sample T.P-6 showed the highest percentage of gypsum. Halite is a deleterious salt that interferes with the integrity of the lime mortar matrix. An increased halite content was registered in samples T.P-6 and T.P-12, while the remaining sample showed negligible amounts. The increased levels of halite in T.P 12 arise due to improper waste water management (from the toilets) in the vicinity of where samples were collected, which leads to the precipitates of salts. Measures were taken to manage the waste water leakages in recent days as the situation is becoming worse. The presence of minerals of the feldspar group originated as aggregates from various rocks.

The plaster samples (T.P-3, T.P-7-10, and T.P-13-15) showed calcite as the main mineral phase with quartz, minerals of the feldspar group, gypsum, halite and traces of kaolinite present. One can observe the existence of gypsum in both bedding and plaster mortars. The gypsum could therefore originate from the source of the binder. Compared to the bedding

Table 4 Results of the acid loss analysis

Sample	Initial weight (g)	Weight of aggregate (g)	Weight of binder (g)	Binder/aggregate
Mud mortar				
T.P-1	28.66	23.21	5.449	1: 4.25
Bedding mortars				
T.P-2	25.51	20.95	4.560	1: 4.59
T.P-4	24.98	19.07	5.911	1: 3.22
T.P-5	25.57	20.09	5.484	1: 3.66
T.P-6	26.46	22.56	3.901	1: 5.78
T.P-11	26.55	21.59	4.963	1: 4.35
T.P-12	24.68	20.84	3.845	1: 5.42
Plaster mortars				
T.P-3	27.41	24.11	3.295	1: 7.31
T.P-7	24.75	20.33	4.420	1: 4.59
T.P-8	27.04	23.75	3.292	1: 7.21
T.P-9	22.82	18.38	4.440	1: 4.13
T.P-10	19.54	16.73	2.810	1: 5.95
T.P-13	26.45	22.25	4.198	1: 5.30
T.P-14	26.51	22.99	3.519	1: 6.53
T.P-15	23.46	19.53	3.935	1: 4.96

mortars, the plaster samples showed a greater precipitation of halite. Halite is a soluble salt which can penetrate lime mortars by moisture transport, and its recrystallization has a negative effect on the microstructure of the mortar [2, 40]. The kaolinite content in plaster mortars can also be described as minimal. In general, the plastered mortars are exposed to an open atmosphere, so the carbonation rate can be good and they harden early compared to bedding mortars. Ancient architects therefore have a profound knowledge of lime hydration chemistry, as can be seen through the different production technologies of bedding and plaster mortars.

3.3 Binder to aggregate ratio

Analysis of the acid loss shows that the binder to aggregate ratio varies between 1: 3.2 and 1: 7.3 throughout the entire structure, which can be seen from the fact that they used different production technologies for bedding and plaster mortars. (Table 4). In the conservation and restoration of ancient lime mortars, the development of a suitable compatible material is of great importance. One parameter which affects the strength of lime mortars is the binder to aggregate ratio. The binder to aggregate ratio of bedding mortars (T.P-2, 4, 5, 6, 11, and 12) was low in the range of 1: 3.2–1: 5.4. Samples T.P-6 and T.P-12 had ratios of 1: 5.8 and 1: 5.4, respectively, which is similar to the loss of binder content, which could be caused by greater precipitation of gypsum and halite salt which was validated by XRD analysis.

Furthermore, the plaster mortars T.P-7 and T.P-9 are in a good state with a binder to aggregate ratio of 1: 4. According to Cazalla et al. [41], an increase in binder to aggregate ratio leads to the formation of fissures, and 1:4 is a common ratio to encounter such fissures. Samples T.P-3, 8, 10 and T.P-13-15 revealed binder to aggregate ratios of 1: 5–1: 7, which

shows that these mortars are in a state of deterioration. Examining the XRD results of the plaster samples (T.P-3, 8, 13 and 15), it can be confirmed that these mortars have the highest precipitation of halite salt. Microscopy showed that sample T.P-15 contains carbonate grains, still the binders are dissolute by acid and consequently higher binder values were seen in this sample. Sample T.P-15 contains carbonate grains, as shown by microscopy, but the carbonate grains are degraded due to acid dissolution resulting in higher binder to aggregate values. The remaining plaster mortars have deteriorated due to an improper drainage system and interaction with atmospheric environmental cycles which leads to the precipitation of halite. The halite percentage is lower in samples T.P-10 and T.P-14, but these mortars may have been damaged by erosion.

The plastered mortars are continuously exposed to atmospheric cycles, so the halite salt originates from the environment. Vitruvius [14] stated that 1:3 is the optimum ratio for the repair of historic mortar, as it leads to an improved carbonation process. From the acid loss test, it can therefore be seen that the physical state of the mortars is of a moderate condition.

3.4 Chemical composition of the binder fraction

Chemical analysis of both bedding and plaster binders showed that CaO and MgO are present as binders with 23% clay impurities. The HI and CI values of calculated lime mortars have displayed weak to moderately hydraulic due to a lower silica content. Aluminum oxide (Al_2O_3) and iron oxide (Fe_2O_3) dominate in the clay minerals, followed by silica oxide (Table 5). Elert et al. [42] discussed the role of magnesium content in lime mortars. He recommended that their presence helps to improve properties such as workability, plasticity, and water retention. The magnesium content of about 13% in the binders at Thanjavur Palace could be a reason for the longevity of the structure. In addition, the higher percentages could cause the mortars to be of poor quality. According to geological data of the Thanjavur district, minerals such as limestone, kankar and laterite soil predominate [38]. In this particular region these mineral deposits are arranged in layers. The higher content of aluminum, iron oxides and the presence of potassium in lime mortars could be due to the fact that the calcined limestone contains clay impurities from laterite soil and kankar. Deleterious compounds such as sulfates (1–8%) and chlorides (1–5%) are also identified in the mortar samples. The presence of sulfates is observed in all samples. Sulfates come from the atmosphere, where they interact with lime and form gypsum. The presence of chloride ions is also observed in all mortars, which could be a result of the poor waste water management system at the palace. Loss of ignition (LOI) was between 21.53 and − 30% (400 °C), which is similar to mortar samples containing volatile substances, i.e., organic compounds. The addition of organic extracts in ancient structures is common practice in India [26, 31]. The uniformity of the LOI values also shows the optimized construction methodology which was used by the ancients in the construction of the structure.

Alkali values ranged from 0.99 to 1.55% and from the value below detection limit to 10.20% for Na_2O and K_2O, respectively. Na_2O is related to the plagioclases and halite found in the samples. The amount of K_2O was higher in the bedding than the plastering mortars, however, mainly due to the kaolinite found in these samples, in addition to K-feldspar. Increased K_2O values were determined for the clay mortar T.P-1.

3.5 Particle size distribution

The particle size distribution of bedding and mortar samples (T.P-1−T.P-15) is shown in Fig. 9. In general, the carbonation of lime-based mortars depends on three main aspects,

Table 5 Chemical compositions of the binders (wt.%)

Sample	CaO	MgO	SO_4^{2-}	Cl^-	Fe_2O_3	Al_2O_3	SiO_2	Na_2O	K_2O	LOI	HI	CI
T.P-1	44.56	11.51	8.91	1.14	9.09	7.61	5.19	1.39	10.2	31.24	0.39	0.52
Bedding mortars												
T.P-2	36.32	11.12	1.53	0.89	10.89	9.76	4.65	1.02	1.79	33.61	0.53	0.66
T.P-4	49.15	13.38	2.33	0.77	7.28	6.95	4.41	1.11	1.59	29.22	0.29	0.40
T.P-5	37.98	14.07	3.27	0.64	8.71	8.26	5.47	1.05	5.58	35.47	0.43	0.58
T.P-6	36.06	12.68	8.70	4.92	9.45	10.94	4.47	0.99	1.74	21.53	0.51	0.63
T.P-11	46.42	11.25	1.10	0.22	9.12	9.72	5.12	1.22	2.52	32.13	0.41	0.54
T.P-12	43.41	13.12	1.61	3.43	10.25	8.91	4.82	1.41	1.32	31.56	0.42	0.53
Plastered mortars												
T.P-3	42.95	13.25	1.65	4.20	11.57	7.84	4.01	1.27	0.46	25.71	0.41	0.49
T.P-7	39.69	12.56	1.04	3.43	8.59	7.93	4.63	1.55	0.00	23.81	0.40	0.53
T.P-8	41.13	15.14	1.15	3.33	12.01	9.66	3.98	1.37	0.00	28.91	0.45	0.53
T.P-9	43.39	10.38	1.45	0.69	9.27	6.96	4.13	1.12	0.10	26.06	0.37	0.47
T.P-10	47.49	12.55	2.76	0.26	7.81	4.74	4.41	1.27	0.10	31.75	0.28	0.38
T.P-13	43.41	13.12	2.20	3.43	10.25	8.91	4.82	1.41	0.20	31.56	0.42	0.53
T.P-14	42.61	14.20	1.10	0.32	11.21	6.78	4.56	1.32	0.00	28.82	0.39	0.49
T.P-15	41.50	12.20	1.10	3.56	8.13	8.62	4.32	1.28	0.20	29.18	0.39	0.50

namely the diffusion of CO_2, the dissolution of portlandite and CO_2, and the formation of stable calcium carbonate. The porosity of lime mortars is the key parameter influencing the diffusion of CO_2. Cultrone et al. [43] found that the total porosity and pore size distribution of lime mortars is strongly dependent on the size and gradation of the aggregates. They also suggested that aggregate is most suitable for lime mortar when it is partially angular, as this enables good interlocking of the grains and reduces porosity.

The gradation curves of all samples confirmed that the aggregates are uniformly graded in nature. Thriumalini et al. [31] investigated the production technology of lime mortars used to construct the ancient structure of the Vadakkumnathan temple in Kerala, India. She discussed the grinding as an alternative technique to improve the slaking and pozzolanic activity of lime. During grinding, the colloidal lime particles are split, and the grain size of siliceous aggregates is reduced to finer particles [41, 44]. It also improves the rate of reaction of mechanisms in lime mortars without disturbing the microstructure. In general, the locally extracted river sand is of a coarse texture, so grinding would have contributed to its partial angular obscuration. The particle size distribution of the mortar sample showed that all particles between 1.18 and 0.3 mm are included. Optical microscopy pictures also confirmed that the shape of the grains is circular to semi-angular.

3.6 Organic content

The presence of biomolecules in the form of carbohydrates, proteins and fats was estimated by an organic test, and their contents are shown in Fig. 10. The results showed that the mortar samples examined were rich in carbohydrates (7–12%), with lower amounts of protein (0.3–3.0%) and fat (0.03–0.3%). The addition of plant extracts to lime mortars in ancient structures was common practice in India [28]. To learn more about the details of the plant

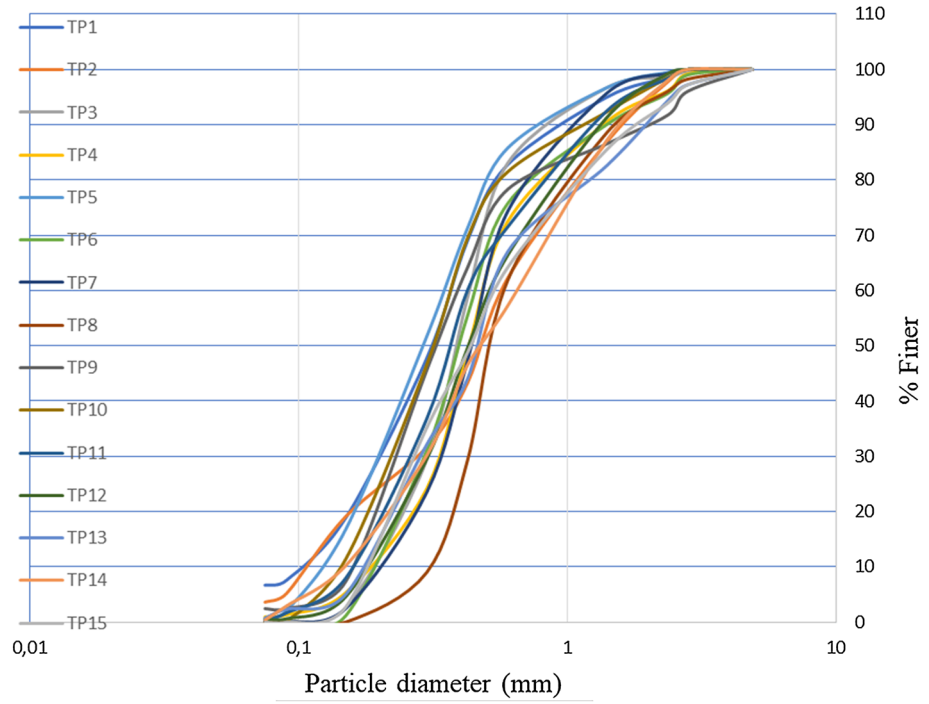

Fig. 9 Particle size distribution of the investigated mortars

extracts used in lime mortars at the Thanjavur Palace, a semi-informal interview was conducted with Sathapathis (who has worked in temples in the area surrounding the palace for generations). They confirmed that it was common practice to add fermented jaggery (*unrefined sugar*) and kadukkai (*Terminalia chebula*) to lime mortars over a period of 7–14 days in the conservation and restoration of ancient structures in the region where the palace is located. In general, kadukkai (local name in Tamil Nadu, India) is dry seed rich in carbohydrates obtained from *Terminalia chebula* tree, and it belongs to Combretaceae family, native to South Asia, most extensively used as Ayurveda medicine in India and grows in any soil type. The regular practice of using lime mortar with jaggery and kadukkai plant extracts is still used for weathering materials naturally.

During fermentation, carbohydrates split into simple sugar compounds, releasing CO_2, and later the sugars are converted into alcohols and acids. Ravi & Thirumalini [45] studied the interaction of fermented organic extract (Cissus glauca roxb) with lime mortars. They found that the organic substances are degraded by microorganisms or enzymes during fermentation, by converting complex compounds into simple substances. The end product produced, alcohol, helps to dissolute the lime particles faster, and CO_2 promotes the carbonation of lime mortars when the mortar is not exposed to the atmosphere. The natural method of adding fermented organic substances could therefore be used specifically to improve the properties of lime mortars.

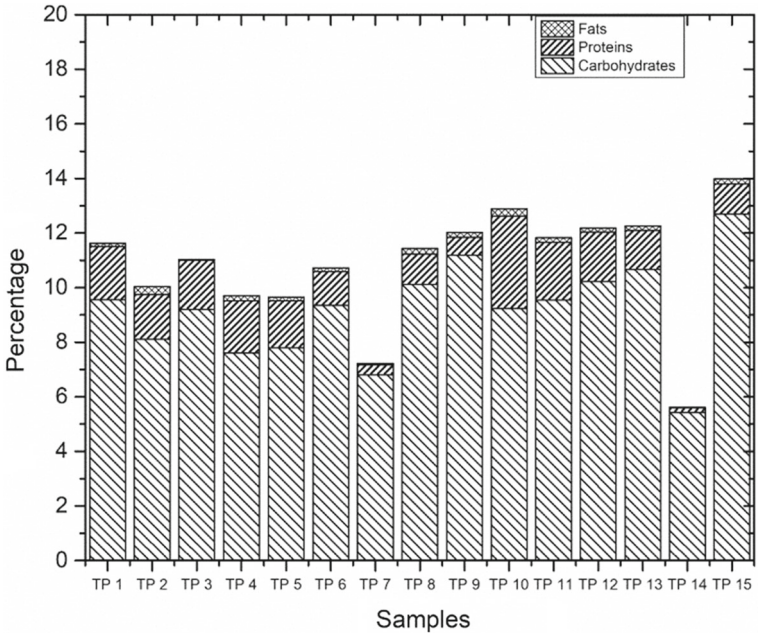

Fig. 10 Organic components in the mortars investigated

4 Conclusions

Mortar samples were taken from a number of sites across Thanjavur Palace, India and chemically investigated (or analyzed) to reproduce the lime mortars for conservation–restoration work. The conclusions reached are.

- The binder, lime used in the current study is pertained to moderately–weakly hydraulic in nature.
- Aggregate grains are attained in rounded, semi-angular and angular forms.
- All the mortars contain quartz as the primary aggregate, with traces of feldspar group also present.
- Binder to aggregate of 1: 3–5 is maintained in the bedding mortars, whereas 1:4–7 is observed in plaster mortars.
- Optical microscopy images of samples have shown that reprecipitation of calcium carbonate has occurred in the mortars
- A greater presence of kaolinite was seen in the bedding mortars compared to the plaster mortars.
- Gypsum is present across both the bedding and plaster mortars.
- Plaster mortars are greatly deteriorated due to the precipitation of halite salt.
- Particle size distribution showed that the grain size of the aggregate is confined to the range 1.18–0.3 mm, which could be due to grinding of the lime mortars.
- The organic tests conducted confirm the presence of plant extracts in the form of carbohydrates, proteins, and fats. These biomolecules acted as chemical admixtures to improve the properties of the mortars investigated.
- Through semi-formal interview, it was confirmed that the addition of fermented plant extracts jaggery and kadukkai in lime mortar samples.

By consolidating the above discussed results, authors have recommended the restoration plan for preparation of lime mortars. Initially, the preparation starts with the selection of raw materials. Moderately hydraulic lime is chosen as binder and procured from local vendors. River sand (passing through 2.36 mm sieve) is incorporated as fine aggregates. Later 1: 3 (binder: aggregate) ratio is preferred as that could be a proven combination for the greater carbonation of lime mortars. Later, 5% (w/v) individual weights of jaggery and kadukkai (combinedly fermented for 14 days) is used as natural admixture in the preparation of lime mortars. The prepared fermented extract is mixed with binder and sand combination and grinded homogenously to attain a fine paste (10 min of grinding). After, the obtained mixture is used as bedding/plaster mortar. For better understanding on the percentage of plant extracts and grinding period, readers could refer the author's pervious works [46, 47].

Acknowledgements The authors acknowledge financial support from the Slovenian Research Agency (research core funding No. P2−0273 and P1-0195)

Data availability This manuscript has associated data in a data repository. [Authors' comment: This manuscript has no associated data or the data will not be deposited.]

Declarations

Conflict of interest No potential conflict of interest was reported by the authors.

References

1. D. Carran, J. Hughes, A. Leslie, C. Kennedy, A short history of the use of lime as a building material beyond Europe and North America. Int. J. Architect. Heritage **6**(2), 117–146 (2012). https://doi.org/10.1080/15583058.2010.511694
2. R.P.J. Van Hees, L. Binda, I. Papayianni, E. Toumbakari, Characterisation and damage analysis of old mortars. Mater. Struct. **37**(273), 644–648 (2004)
3. A. Arizzi, G. Cultrone, Aerial lime-based mortars blended with a pozzolanic additive and different admixtures: a mineralogical, textural and physical-mechanical study. Constr. Build. Mater. **31**, 135–143 (2012). https://doi.org/10.1016/j.conbuildmat.2011.12.069
4. I. Papayianni, M. Stefanidou, Durability aspects of ancient mortars of the archeological site of Olynthos. J. Cult. Herit. **8**(2), 193–196 (2007). https://doi.org/10.1016/j.culher.2007.03.001
5. A. Moropoulou, A. Bakolas, S. Anagnostopoulou, Composite materials in ancient structures. Cem. Concr. Compos. **27**(2), 295–300 (2005). https://doi.org/10.1016/j.cemconcomp.2004.02.018
6. S. Sánchez-Moral, L. Luque, J.C. Canaveras, V. Soler, J. Garcia-Guinea, A. Aparicio, Lime–pozzolana mortars in Roman catacombs: composition, structures and restoration. Cement Concr. Res. **35**(8), 1555–1565 (2005). https://doi.org/10.1016/j.cemconres.2004.08.009
7. M.D. Jackson, S.R. Chae, S.R. Mulcahy, C. Meral, R. Taylor, P. Li, A.H. Emwas, J. Moon, S. Yoon, G. Vola, H.R. Wenk, Unlocking the secrets of Al-tobermorite in Roman seawater concrete. Am. Miner. **98**(10), 1669–1687 (2013). https://doi.org/10.2138/am.2013.4484
8. M.D. Jackson, J. Moon, E. Gotti, R. Taylor, S.R. Chae, M. Kunz, A.H. Emwas, C. Meral, P. Guttmann, P. Levitz, H.R. Wenk, Material and elastic properties of Al-tobermorite in ancient Roman seawater concrete. J. Am. Ceram. Soc. **96**(8), 2598–2606 (2013). https://doi.org/10.1111/jace.12407
9. M.D. Jackson, S.R. Mulcahy, H. Chen, Y. Li, Q. Li, P. Cappelletti, H.R. Wenk, Phillipsite and Al-tobermorite mineral cements produced through low-temperature water-rock reactions in Roman marine concrete. Am. Miner. **102**(7), 1435–1450 (2017). https://doi.org/10.2138/am-2017-5993CCBY
10. S. Kramar, V. Zalar, M. Urosevic, W. Körner, A. Mauko, B. Mirtič, J. Lux, A. Mladenović, Mineralogical and microstructural studies of mortars from the bath complex of the Roman villa rustica near Mošnje (Slovenia). Mater. Charact. **62**(11), 1042–1057 (2011). https://doi.org/10.1016/j.matchar.2011.07.019

11. E. Uğurlu, H. Böke, The use of brick–lime plasters and their relevance to climatic conditions of historic bath buildings. Constr. Build. Mater. **23**(6), 2442–2450 (2009). https://doi.org/10.1016/j.conbuildmat.2008.10.005
12. P. Maravelaki-Kalaitzaki, A. Bakolas, I. Karatasios, V. Kilikoglou, Hydraulic lime mortars for the restoration of historic masonry in Crete. Cement Concr. Res. **35**(8), 1577–1586 (2005). https://doi.org/10.1016/j.cemconres.2004.09.001
13. H. Böke, S. Akkurt, B. İpekoğlu, E. Uğurlu, Characteristics of brick used as aggregate in historic brick-lime mortars and plasters. Cement Concrete Res. **36**(6), 1115–1122 (2006). https://doi.org/10.1016/j.cemconres.2006.03.011
14. P. Vitruvius, Ten books on architecture. (Translation by Ingrid D. Rowland, 2001).
15. E. Vejmelková, M. Keppert, P. Rovnaníková, Z. Keršner, R. Černý, Application of burnt clay shale as pozzolan addition to lime mortar. Cement Concr. Compos. **34**(4), 486–492 (2012). https://doi.org/10.1016/j.cemconcomp.2012.01.001
16. L.B. Sickels, Mortars in Old buildings and in Masonry conservation: a historical and practical treatise (Doctoral dissertation, The University of Edinburgh (United Kingdom)) (1988)
17. D.S. Mitchell, The use of lime and cement in traditional buildings (2007)
18. F. Yang, B. Zhang, C. Pan, Y. Zeng, Traditional mortar represented by sticky rice lime mortar—one of the great inventions in ancient China. Sci. China Ser. E: Technol. Sci. **52**(6), 1641–1647 (2009). https://doi.org/10.1007/s11431-008-0317-0
19. F. Yang, B. Zhang, Q. Ma, Study of sticky rice−lime mortar technology for the restoration of historical masonry construction. Acc. Chem. Res. **43**(6), 936–944 (2010). https://doi.org/10.1021/ar9001944
20. C. Fiori, M. Vandini, S. Prati, G. Chiavari, Vaterite in the mortars of a mosaic in the Saint Peter basilica, Vatican (Rome). J. Cult. Heritage **10**(2), 248–257 (2009). https://doi.org/10.1016/j.culher.2008.07.011
21. Y. Zeng, B. Zhang, X. Liang, A case study and mechanism investigation of typical mortars used on ancient architecture in China. Thermochim. Acta **473**(1–2), 1–6 (2008). https://doi.org/10.1016/j.tca.2008.03.019
22. S. Fang, H. Zhang, B. Zhang, G. Li, A study of Tung-oil–lime putty—a traditional lime-based mortar. Int. J. Adhesion Adhesives **48**, 224–230 (2014). https://doi.org/10.1016/j.ijadhadh.2013.09.034
23. C. Nunes, Z. Slížková, Hydrophobic lime-based mortars with linseed oil: characterization and durability assessment. Cem. Concr. Res. **61**, 28–39 (2014). https://doi.org/10.1016/j.cemconres.2014.03.011
24. L. Ventolà, M. Vendrell, P. Giraldez, L. Merino, Traditional organic additives improve lime mortars: new old materials for restoration and building natural stone fabrics. Constr. Build. Mater. **25**(8), 3313–3318 (2011). https://doi.org/10.1016/j.conbuildmat.2011.03.020
25. S. Thirumalini, Heritage lime mortar characterisation and simulation (2015)
26. R. Ravi, S. Thirumalini, N. Taher, Analysis of ancient lime plasters–Reason behind longevity of the Monument Charminar, India a study. J. Build. Eng. **20**, 30–41 (2018). https://doi.org/10.1016/j.jobe.2018.04.010
27. A.S. Nene, Building materials and construction techniques of ancient India. New Delhi, India, Ganga (2012)
28. S. Chandra, *History of Architecture and Ancient Building Materials in India: Part I & Part II (in Single Volume)* (Tech Books Int, New Delhi, 2003)
29. S. Pradeep, T. Selvaraj, Identification of bio-minerals and their origin in lime mortars of ancient monument: Thanjavur Palace. Int. J. Architect. Heritage **15**(3), 426–436 (2019). https://doi.org/10.1080/15583058.2019.1623341
30. F.M. León-Martínez, P.D.J. Cano-Barrita, F. Castellanos, K.B. Luna-Vicente, S. Ramírez-Arellanes, C. Gómez-Yáñez, Carbonation of high-calcium lime mortars containing cactus mucilage as additive: a spectroscopic approach. J. Mater. Sci. **56**(5), 3778–3789 (2021). https://doi.org/10.1007/s10853-020-05514-5
31. S. Thirumalini, R. Ravi, S.K. Sekar, M. Nambirajan, Knowing from the past–ingredients and technology of ancient mortar used in Vadakumnathan temple, Tirussur, Kerala, India. J. Build. Eng. **4**, 101–112 (2015). https://doi.org/10.1016/j.jobe.2015.09.004
32. B. Middendorf, J.J. Hughes, K. Callebaut, G. Baronio, I. Papayianni, Investigative methods for the characterisation of historic mortars—part 2: chemical characterisation. Mater. Struct. **38**(8), 771–780 (2005). https://doi.org/10.1007/BF02479290
33. E.C. Eckel, *Cements, Limes and Plaster* (Routledge, 2015)
34. H.F. Taylor, *Cement Chemistry*, vol. 2 (Thomas Telford, London, 1997)
35. IS:2386 (Part I)—1975. Method of Test for Aggregate and Concrete-Particle Size and Shape. Bureau of Indian Standard, New Delhi, India (1991)
36. IS:7874 (Part I)—1975. Methods of Tests for Animal Feeds and Feeding Stuffs. Bureau of Indian Standard, New Delhi, India (1991)

37. K.M. Haneefa, S.D. Rani, R. Ramasamy, M. Santhanam, Microstructure and geochemistry of lime plaster mortar from a heritage structure. Constr. Build. Mater. **225**, 538–554 (2019). https://doi.org/10.1016/j.conbuildmat.2019.07.159
38. V. Selvakumar, Prehistoric and historical archaeology of the lower Kaviri Valley and Pudukottai Region, Tamil Nadu, in *Proceedings of the Indian History Congress,* vol 69, (2008), pp. 1015–1023 (2008). Indian History Congress. https://www.jstor.org/stable/44147262
39. B. Lubelli, T.G. Nijland, R.P.J. Van Hees, Self-healing of lime-based mortars: microscopy observations on case studies. Heron **56** (1/2) (2011)
40. J.M.P.Q. Delgado, A.S. Guimarães, V.P. De Freitas, I. Antepara, V. Kočí, R. Černý, Salt damage and rising damp treatment in building structures. Adv. Mater. Sci. Eng. (2016). https://doi.org/10.1155/2016/1280894
41. O. Cazall, C. Rodriguez-Navarro, E. Sebastian, G. Cultrone, M.J. De la Torre, Aging of lime putty: effects on traditional lime mortar carbonation. J. Am. Ceramic Soc. **83**(5), 1070–1076 (2000). https://doi.org/10.1111/j.1151-2916.2000.tb01332.x
42. K. Elert, C. Rodriguez-Navarro, E.S. Pardo, E. Hansen, O. Cazalla, Lime mortars for the conservation of historic buildings. Stud. Conserv. **47**(1), 62–75 (2002). https://doi.org/10.1179/sic.2002.47.1.62
43. G. Cultrone, E. Sebastián, M.O. Huertas, Forced and natural carbonation of lime-based mortars with and without additives: mineralogical and textural changes. Cem. Concr. Res. **35**(12), 2278–2289 (2005). https://doi.org/10.1016/j.cemconres.2004.12.012
44. A. Moropoulou, A. Cakmak, K.C. Labropoulos, R. Van Grieken, K. Torfs, Accelerated microstructural evolution of a calcium-silicate-hydrate (CSH) phase in pozzolanic pastes using fine siliceous sources: comparison with historic pozzolanic mortars. Cement Concrete Res. **34**(1), 1–6 (2004). https://doi.org/10.1016/S0008-8846(03)00187-X
45. R. Ravi, S. Thirumalini, Effect of natural polymers from cissus glauca roxb on the mechanical and durability properties of hydraulic lime mortar. Int. J. Architect. Heritage **13**(2), 229–243 (2019). https://doi.org/10.1080/15583058.2018.1431732
46. R. Ramadoss, A. Ahamed, T. Selvaraj, Alternative approach for traditional slaking and grinding of air lime mortar for restoration of heritage structures: natural polymer. J. Architect. Eng. **25**(3), 04019017 (2019). https://doi.org/10.1061/(ASCE)AE.1943-5568.0000361
47. S. Jayasingh, T. Selvaraj, Effect of natural herbs on hydrated phases of lime mortar. J. Architect. Eng. (2020). https://doi.org/10.1061/(ASCE)AE.1943-5568.0000420